Article ID: 1007-4627(2015) 04-0405-05

Comparison Between the First Iteration of the Self-consistent Soliton Solution with Different Initial Chiral Angle in the Chiral Quark Soliton Model

JIANG Xuemin, LI Yunde

(*Department of Physics, Yunnan University, Kunming 650091, China*)

Abstract: We use three different initial chiral angles to give the solution of the mean-field equation of the system with baryon number $B=1$ for the first iteration, to investigate which initial chiral angle will make the self-consistency reach faster. From the first iteration from different initial chiral angle, we found that the result from the exponential form chiral angle is closer to the self-consistent one than the other two initial chiral angles.

Key words: self-consistent soliton solution; chiral quark soliton model; chiral angle

CLC number: O532.33 **Document code:** A **DOI:** 10.11804/NuclPhysRev.32.04.405

1 Introduction

The chiral quark soliton model is one of QCD effective theories incorporating the spontaneous chiral symmetry breaking of the low-energy QCD[1]. It includes both valence quark degree of freedom and the contribution from Dirac sea quarks. The two flavor Lagrangian of the chiral quark soliton model is

$$L_{\mathrm{M}}=\bar{q}(x)\mathrm{i}Dq(x) , \tag{1}$$

where iD is

$$\mathrm{i}D=\mathrm{i}\,\partial\!\!\!/-M(\sigma+\mathrm{i}\boldsymbol{\pi}\boldsymbol{\tau}\gamma_5) , \tag{2}$$

M is the only free parameter of the model. It is the constituent quark mass.

It is worthwhile to investigate which initial profile function will make the self-consistent determination process consuming less time. We investigate the first iteration profile function $P(r)$ using three different initial chiral angles to see which resultant $P(r)$ after the first iteration is the closest to the self-consistent one to gain some insight into this problem.

Those three chiral angles are:

(1) a linear form[2]

$$P(r)=\frac{-n\pi}{R}r-\pi,(0\leqslant r\leqslant R) , \tag{3}$$

(2) an exponential form[3]:

$$P(r)=-n\pi\mathrm{e}^{-\frac{r}{R}} , \tag{4}$$

(3) an inverse trigonometric form[1]

$$P(r)=-2n\arctan(\frac{R}{r})^2 , \tag{5}$$

where n is the topological winding number and R characterizes the size of the meson profile[4]. The chiral angle should satisfy the boundary conditions[1]:

$$P(\infty)\to 0 , \quad P(0)\to -\pi . \tag{6}$$

These three chiral angles are plotted in Fig. 1.

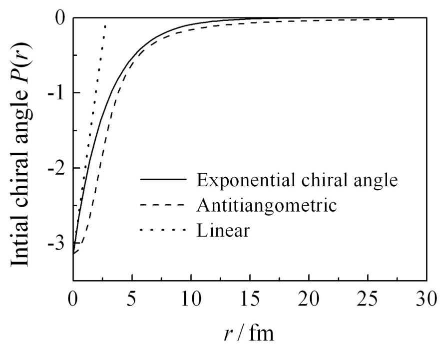

Fig. 1 Three different initial chiral angles.
Including the linear form (dotted line), the exponential form(solid line), and the inverse trigonometric form (dashed-line).

Received date: 13 Apr. 2015; **Revised date:** 15 May 2015

Foundation item: National Natural Science Foundation of China(11465021, 11065010)

Biography: JIANG Xuemin(1988–), female, Kunming, Yunnan, postgraduate, working on the field of theoretical physics: particle physics and nuclear physics; E-mail: jxmhh0926@126.com

Corresponding author: LI Yunde, E-mail: yndxlyd@163.cm.

This article is organized as followed: In Sect. 2 we introduce how the field equations for meson fields are derived. In Sect. 3, we present the first iteration result of the field equation from the three initial chiral angles. The conclusions are reserved in Sect. 4.

2 The field equations for meson fields

The vacuum functional of the chiral quark soliton model is[1]:

$$Z = \int D\pi D q D\bar{q} \exp[\mathrm{i}\int \mathrm{d}^4 x \bar{q}(\mathrm{i}\,\partial\!\!\!/ - MU^{\gamma^5})q] \ . \quad (7)$$

After integrating over the fermion fields q and $\bar{q}$, one obtains the effective action:

$$\begin{aligned} S_{\mathrm{eff}} &= -\mathrm{Spln}(-\mathrm{i}D) = -\mathrm{lndet}(-\mathrm{i}D) \\ &= -\mathrm{lndet}[\beta(\frac{\partial}{\partial\tau} + h)] \ , \end{aligned} \quad (8)$$

where h denotes the single quark hamiltonian, such that:

$$\begin{aligned} h &= \frac{\boldsymbol{\alpha}\cdot\boldsymbol{\nabla}}{\mathrm{i}} + M\beta(\sigma(\boldsymbol{r}) + \mathrm{i}\boldsymbol{\pi}(\boldsymbol{r})\boldsymbol{\tau}\gamma_5) \ , \\ h\phi_\lambda(\boldsymbol{r}) &= E_\lambda \phi_\lambda(\boldsymbol{r}) \ . \end{aligned} \quad (9)$$

The classical energy of the soliton can be estimated from the quark determinant in Eq. (8)[5]. It can be written as:

$$E_{\mathrm{classical}} = E_{\mathrm{val}} + E_{\mathrm{vacum}} \ , \quad (10)$$

E_{val} is the valence quark energy contribution and E_{vacum} is the sea quarks energy contribution.

Because the effective action is ultraviolet divergent and it can be regularized using a proper-time regularization such that[6–7]:

$$\begin{aligned} S_{\mathrm{eff}}^{\mathrm{reg}} &= \frac{\mathrm{i}}{2} N_{\mathrm{c}} T \int_{-\infty}^{+\infty} \frac{\mathrm{d}w}{2\pi} \int_{1/\Lambda^2}^{+\infty} \frac{\mathrm{d}\tau}{\tau} \times \\ &\quad \mathrm{Sp}\left[\mathrm{e}^{-\tau(h^2+w^2)} - \mathrm{e}^{-\tau(h_0{}^2+w^2)}\right] \ , \end{aligned} \quad (11)$$

the total energy is then given as:

$$\begin{aligned} E_{\mathrm{soliton}} &= E_{\mathrm{val}}[P(r)] + E_{\mathrm{vacum}}[P(r)] - E_{\mathrm{vacum}}[P(r)=0] \\ &= N_{\mathrm{c}} E_{\mathrm{val}} + \frac{\Lambda}{4\sqrt{\pi}} N_{\mathrm{c}} \int_1^{+\infty} \frac{\mathrm{d}s}{s^{3/2}} \times \\ &\quad \left[\sum_\lambda \mathrm{e}^{-s(E_\lambda/\Lambda)^2} - \sum_\lambda \mathrm{e}^{-s(E_{\lambda_V}/\Lambda)^2}\right] \ . \end{aligned} \quad (12)$$

Λ is also a parameter of the chiral quark soliton model, coming from the Proper-time regularization which can be set as 650 MeV[8]. M denotes the constituent quark mass, which can be set as 420 MeV[8]. E_{λ_V} is the energy of the free single quark hamiltonian, such that:

$$\begin{aligned} h_0 &= \frac{\boldsymbol{\alpha}\cdot\nabla}{\mathrm{i}} + M\beta \ , \\ h\phi_{\lambda_V}(\boldsymbol{r}) &= E_{\lambda_V}\phi_{\lambda_V}(\boldsymbol{r}) \ . \end{aligned} \quad (13)$$

The field equations for meson fields can be obtained by demanding the total energy of the soliton be stationary with respect to variation of the chiral angle $P(r)$[4, 9], such that

$$\delta_{P(r)} E_{\mathrm{soliton}} = 0 \ . \quad (14)$$

This equation can then be simplified to:

$$\sin P(r) S_n(r) = \cos P(r) P_n(r) \ , \quad (15)$$

where

$$\begin{aligned} S_n(r) =& \bar{\phi}_{\mathrm{val}}(r,\Omega)\phi_{\mathrm{val}}(r,\Omega) + \\ & \sum_\lambda (-\frac{1}{\sqrt{4\pi}} \int_1^\infty \mathrm{d}s s^{-1/2} \frac{E_\lambda}{\Lambda} \mathrm{e}^{-s(\frac{E_\lambda}{\Lambda})^2}) \times \\ & \bar{\phi}_\lambda(r,\Omega)\phi_\lambda(r,\Omega) \ , \\ P_n(r) =& \bar{\phi}_{\mathrm{val}}(r,\Omega)(\mathrm{i}\hat{r}\boldsymbol{\tau}\gamma^5)\phi_{val}(r,\Omega) + \\ & \sum_\lambda -\frac{1}{\sqrt{4\pi}} \int_1^\infty \mathrm{d}s s^{-1/2} \frac{E_\lambda}{\Lambda} \mathrm{e}^{-s(\frac{E_\lambda}{\Lambda})^2} \times \\ & \bar{\phi}_\lambda(r,\Omega)(\mathrm{i}\hat{r}\boldsymbol{\tau}\gamma^5)\phi_\lambda(r,\Omega) \ , \end{aligned} \quad (16)$$

$\phi_\lambda(r,\Omega)$ and E_λ are the eigenfunctions and the corresponding eigenvalues of the single particle hamiltonian.

Eq. (14) is solved self-consistenly[9]. The procedure is: (1) solve the eigenequation of the single particle hamiltonian Eq. (9) using an initial profile function $P(r)$. This step is accomplished by using a Kahana-Ripka method which is given in Appendix, (2) a new set of $S_n(r)$ and $P_n(r)$ is obtained using the eigenfunctions and the eigenvalues of the hamiltonian Eq. (9). (3) solve (15) to get the first iteration profile function $P(r)$. (4) repeat (1) to (3) to get the nth iteration $P(r)$ until the satisfying self-consistency is reached.

3 Numerical results and discussions

The first iteration chiral angles from different initial chiral angles are presented in Fig. 2. The first iteration from the linear one has already been given in Ref. [9]. They use Λ/M as the free parameter, which they set it to be 1.4 when calculating the self-consistent profile function. In our work, the value of Λ/M approximately equals to 1.54.

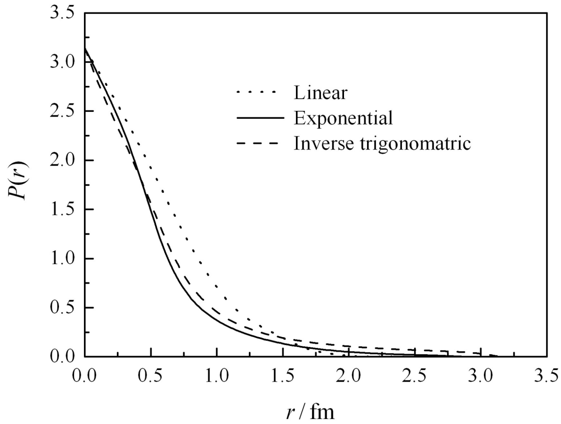

Fig. 2　The first iteration $P(r)$ originating from three different initial chiral angles.
Including an initial linear form (dotted line), an initial exponential form(solid line), an initial inverse trigonometric form (dashed-line).

It is easily seen from the picture that: the first iteration chiral angle from inverse trigonometric chiral angle vanishes after around 3 fm; the one from linear form vanishes after around 2 fm; and the one from exponential form vanishes after around 2.5 fm.

The self-consistent soliton solution after many times iteration has been given in Ref. [3, 9]. In comparison with the more accurate self-consistent soliton solution, it can be seen from Fig. 2 that in the region around $r<0.5$ fm the first iteration self-consistent soliton solution from the initial inverse trigonometric form is closer to the more accurate self-consistent solution; the first iteration self-consistent soliton solution from the initial exponential form is less close to the more accurate self-consistent one; the first iteration self-consistent soliton solution from the initial linear form is the least close one. However, in the region around $3 \geqslant r \geqslant 0.5$ fm it can also be seen from Fig. 2 that the first iteration self-consistent soliton solution from the initial exponential form is closer to the more accurate self-consistent solution; the first iteration self-consistent soliton solution from the initial inverse trigonometric form is less close to the more accurate self-consistent one; the first iteration self-consistent soliton solution from the initial linear form is the least close one. On the whole, the first iteration self-consistent soliton solution from the initial exponential form is closer than the inverse trigonometric one to the more accurate self-consistent solution.

Therefore, we can conclude that if the initial profile function is in the exponential form, the self-consistency will be reached sooner than those in the linear form or the exponential form after the same times of iteration.

4　Conclusions

In conclusion, we investigate how fast the self-consistency of the self-consistent soliton solution for $B=1$ system in the chiral quark soliton model is reached through comparing the first iteration of the self-consistent solution from three different initial chiral angles, including a linear one, an exponential one and an inverse trigonometric one. The results show that the self-consistency of the self-consistent soliton solution reaches faster than the other two chiral angles when using the exponential chiral angle as the initial chiral angle.

In our future work, we will present the more accurate self-consistent soliton solution after many times iteration, and take a more detailed insight into this problem.

5　Appendix: Kahana-Ripka numerical method

The eigenstates of h_0 can be used as a set of complete basis to calculate the eigenvalues of h, which is done by diagonalize h in the basis of the eigenstates of h_0[2], because both h_0 and h commutes with the grand-spin operator $G=J+\tau(J=L+S)$ and the relativistic parity operator $\hat{\prod}$.

According to Ref. [2,8,10], a plane-wave basis is used as the eigenfunction of h_0. They can be divided into natural parity and unnatural parity. The states with natural parity are those with $G^P=0^+,1^-,2^+...(G\neq 0)$. For each $G^P(G\neq 0)$, there are four independent plane-wave solutions

$$\begin{aligned}
\varphi_{\mathrm{a}}^{(n)} &= N_k \begin{pmatrix} \mathrm{i}\,\mathrm{j}_G(kr)\,|0\rangle \\ \dfrac{k}{|\varepsilon_k|+M}\mathrm{j}_{G+1}(kr)\,|2\rangle \end{pmatrix}, \\
\varphi_{\mathrm{b}}^{(n)} &= N_k \begin{pmatrix} \mathrm{i}\,\mathrm{j}_G(kr)\,|1\rangle \\ \dfrac{-k}{|\varepsilon_k|+M}\mathrm{j}_{G-1}(kr)\,|3\rangle \end{pmatrix}, \\
\chi_{\mathrm{a}}^{(n)} &= N_k \begin{pmatrix} \mathrm{i}\dfrac{k}{|\varepsilon_k|+M}\mathrm{j}_G(kr)\,|0\rangle \\ -\mathrm{j}_{G+1}(kr)\,|2\rangle \end{pmatrix}, \\
\chi_{\mathrm{b}}^{(n)} &= N_k \begin{pmatrix} \mathrm{i}\dfrac{k}{|\varepsilon_k|+M}\mathrm{j}_G(kr)\,|1\rangle \\ \mathrm{j}_{G-1}(kr)\,|3\rangle \end{pmatrix}.
\end{aligned} \tag{17}$$

where $\varphi_{\mathrm{a}}^{(n)}$ and $\varphi_{\mathrm{b}}^{(n)}$ are the positive energy solutions with $\varepsilon_k=\sqrt{k^2+M^2}$ and $\chi_{\mathrm{a}}^{(n)}$ and $\chi_{\mathrm{b}}^{(n)}$ are the negative energy solutions with $\varepsilon_k=-\sqrt{k^2+M^2}$.

The unnatural parity states are those with $G^P=0^-,1^+,2^-...(G\neq 0)$, there are also 4 independent solutions for each G^P:

$$\varphi_{\rm a}^{(u)} = N_k \begin{pmatrix} {\rm i}{\rm j}_{G+1}(kr)\,|2\rangle \\ -\dfrac{k}{|\varepsilon_k|+M}{\rm j}_G(kr)\,|0\rangle \end{pmatrix} ,$$

$$\varphi_{\rm b}^{(u)} = N_k \begin{pmatrix} {\rm i}{\rm j}_{G-1}(kr)\,|3\rangle \\ \dfrac{k}{|\varepsilon_k|+M}{\rm j}_G(kr)\,|1\rangle \end{pmatrix} ,$$

$$\chi_{\rm a}^{(u)} = N_k \begin{pmatrix} {\rm i}\dfrac{k}{|\varepsilon_k|+M}{\rm j}_{G+1}(kr)\,|2\rangle \\ {\rm j}_G(kr)\,|0\rangle \end{pmatrix} ,$$

$$\chi_{\rm b}^{(u)} = N_k \begin{pmatrix} {\rm i}\dfrac{k}{|\varepsilon_k|+M}{\rm j}_{G-1}(kr)\,|3\rangle \\ -{\rm j}_G(kr)\,|1\rangle \end{pmatrix} . \qquad (18)$$

where $\varphi_{\rm a}^{(u)}$ and $\varphi_{\rm b}^{(u)}$ are the positive energy solutions with $\varepsilon_k = \sqrt{k^2+M^2}$ and $\chi_{\rm a}^{(u)}$ and $\chi_{\rm b}^{(u)}$ are the negative energy solutions with $\varepsilon_k = -\sqrt{k^2+M^2}$.

The normalization of the plane waves are given by[8]

$$N_k = \left[\frac{2\,|\varepsilon_k|}{M+|\varepsilon_k|}\right]^{-\frac{1}{2}} \left[\sqrt{\frac{D^3}{2}}\left|{\rm j}_{G+1}(kD)\right|\right]^{-1} .$$

The equation below are the angular basis corresponding to the angular momentum coupling scheme[8]:

$$|0\rangle = \left| l=G,\ {\rm j}=G+\frac{1}{2}, GG_3 \right\rangle ,$$

$$|1\rangle = \left| l=G,\ {\rm j}=G-\frac{1}{2}, GG_3 \right\rangle ,$$

$$|2\rangle = \left| l=G+1,\ {\rm j}=G+\frac{1}{2}, GG_3 \right\rangle ,$$

$$|3\rangle = \left| l=G-1,\ {\rm j}=G-\frac{1}{2}, GG_3 \right\rangle . \qquad (19)$$

They form a complete orthogonal basis. According to Ref. [2], the non-vanishing elements of $\langle l'j'GG_3|\hat{\boldsymbol r}\cdot\boldsymbol\tau|ljGG_3\rangle$ are

$$\langle 0|\hat{\boldsymbol r}\cdot\boldsymbol\tau|2\rangle = \langle 2|\hat{\boldsymbol r}\cdot\boldsymbol\tau|0\rangle = \frac{1}{2G+1} ,$$

$$\langle 0|\hat{\boldsymbol r}\cdot\boldsymbol\tau|3\rangle = \langle 3|\hat{\boldsymbol r}\cdot\boldsymbol\tau|0\rangle = \frac{(-2\sqrt{G(G+1)})}{2G+1} ,$$

$$\langle 1|\hat{\boldsymbol r}\cdot\boldsymbol\tau|2\rangle = \langle 2|\hat{\boldsymbol r}\cdot\boldsymbol\tau|1\rangle = \frac{(-2\sqrt{G(G+1)})}{2G+1} ,$$

$$\langle 1|\hat{\boldsymbol r}\cdot\boldsymbol\tau|3\rangle = \langle 3|\hat{\boldsymbol r}\cdot\boldsymbol\tau|1\rangle = \frac{-1}{2G+1} . \qquad (20)$$

For $G'_3 \neq G_3$ or $G' \neq G$, the values are zero.

To calculate the eigenvalues of h, the continuous parameter k has to be discretized by imposing the Kahana-Ripka boundary condition[2]:

$${\rm j}_G(k_n D) = 0 .$$

D is the radius of a spherical box where the system has been put in. It is chosen to be larger than the soliton size. In our work, we set it as $D \approx 6/M$. The basis is made finite by imposing a cut-off $k_{\rm max}$ on the momentum k. It should be noticed that the cut-off $k_{\rm max}$ has no physical meaning and has nothing to do with the momentum cut-off Λ mentioned before. We use the same $k_{\rm max} \approx 7M$ as Ref. [3].

References:

[1] DIAKONOV D I, PETROV Y V, POBYLITSA V P. Nucl Phys B, 1988, **306**: 809.

[2] KAHANA S, RIPKA G. Nucl Phys A, 1984, **429**: 462.

[3] CHRISTOV V C, BLOTZ A, KIM H C, *et al.* Prog Part Nucl Phys, 1996, **37**: 91.

[4] MEISSNER T H, ARRIOLA E R, BLOTZ A. arVix:hep-ph/9401216, 1994.

[5] ARRIOLA R, ALBERTO P E, URBANO J N, *et al.* Z Phys A, 1989, **333**: 203.

[6] SCHWINGER J. Phys Rev, 1951, **82**: 664.

[7] SAWADO N, SHIIKI N. arXiv:hep-ph/0204198VI, 2002.

[8] LEDWIG T. Anti-Decuplet Pentaquarks in the Chiral Quark-Soliton Model[D]. Bochum: Ruhr-University, 2007(12), 153.

[9] REINHARDT H, WUNSCH R. Phys Lett B, 1988, **215**: 577.

[10] WAKAMATSU M, YOSHIKI H. Nucl Phys A, 1991, **524**: 561.

由 3 个不同的初始手征角给出的初次迭代后的自洽手征孤子解

江学敏，李云德

(云南大学物理科学技术学院，昆明 650091)

摘要： 利用 3 个不同的初始手征角，给出了重子数为 1 的体系的平均场方程的一次迭代后的解，以此研究哪一种手征角可以令平均场方程的解的自洽性更快地达到。对于不同的初始手征角，发现经过第一次迭代后，指数形式的手征角给出的结果比别的手征角更接近自洽解的形状。

关键词： 自洽孤子解；手征夸克孤子模型；手征角

收稿日期： 2015-04-13；　**修改日期：** 2015-05-15

基金项目： 国家自然科学基金资助项目(11465021, 11065010)

通信作者： 李云德，E-mail: yndxlyd@163.com。